

1 Supporting Information

2 Figures S1–S15.

3 Mesophase-Mediated Crystallization of Poly(L-lactide): 4 Deterministic Pathways to Nanostructured Morphology and 5 Superstructure Control

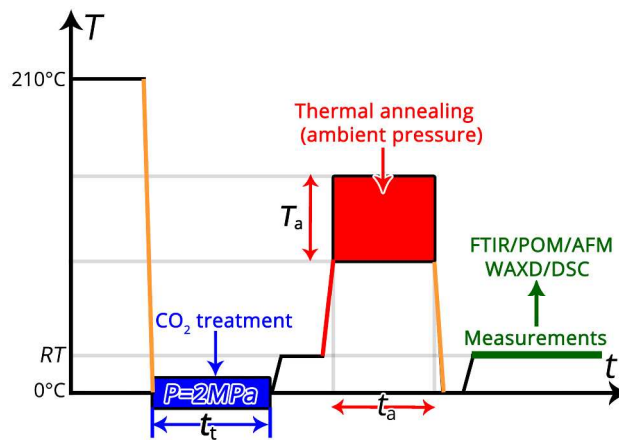
6 *Qiaofeng Lan,* and Yong Li*

7 Ningbo Institute of Materials Technology and Engineering, Chinese Academy of Sciences
8 (CAS), Ningbo 315201, China

9 * Corresponding authors.

10 E-mail address: lanqf@nimte.ac.cn or lanqf2016@gmail.com (Q.L.).

11

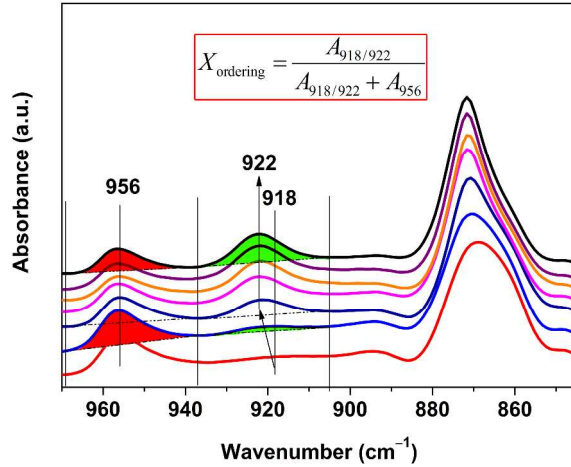


12

13 **Figure S1.** Temperature-time protocol for the CO₂ treatment at 2 MPa/ $T_t = 0$ °C for $t_t = 15$ s–360

14 min and/or subsequent thermal annealing at $T_a = 78$ –135 °C under atmospheric pressure for $t_a =$

15 5 s–1 h.

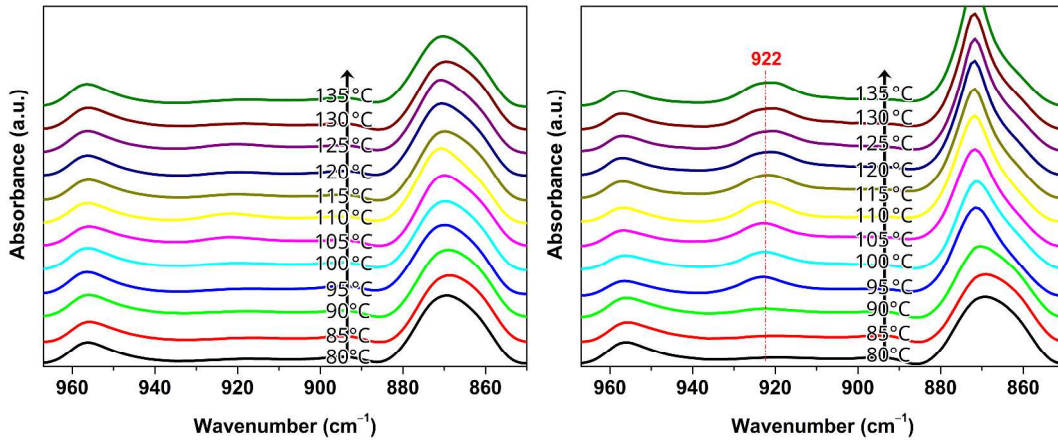


1
 2 **Figure S2.** Calculation of the overall fraction of the structural ordering (X_{ordering}) including the
 3 crystal (with 922 cm^{-1} band) (X_{crystal}) and/or mesophase (with 918 cm^{-1} band), and intermediate
 4 (with band at range of $918\text{--}922\text{ cm}^{-1}$) structure having degree of conformational ordering
 5 between mesophase and crystal, were performed according to the equation (inset)^{1,2} as follows

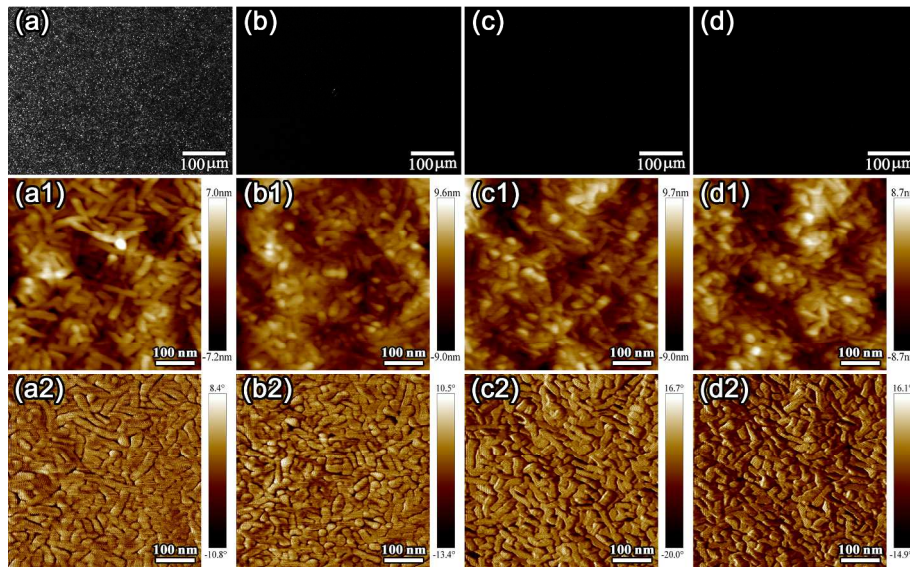
6
$$X_{\text{ordering}} = \frac{A_{918/922}}{A_{918/922} + A_{956}}$$

7 where $A_{918/922}$ and A_{956} are the integrated intensities (as shown by the representative shadows) of
 8 the IR bands at around $918\text{ to }922\text{ cm}^{-1}$ and 956 cm^{-1} , respectively. The equation was applied to
 9 the calculation for the FTIR spectra in Figures 1–3, Figure 9b, and Figure 11. When the
 10 crystalline phase (showed 922 cm^{-1} band) was exclusively and definitely present in the PLLA
 11 sample, the X_{ordering} was expressed as X_{crystal} .

12
 13
 14
 15
 16

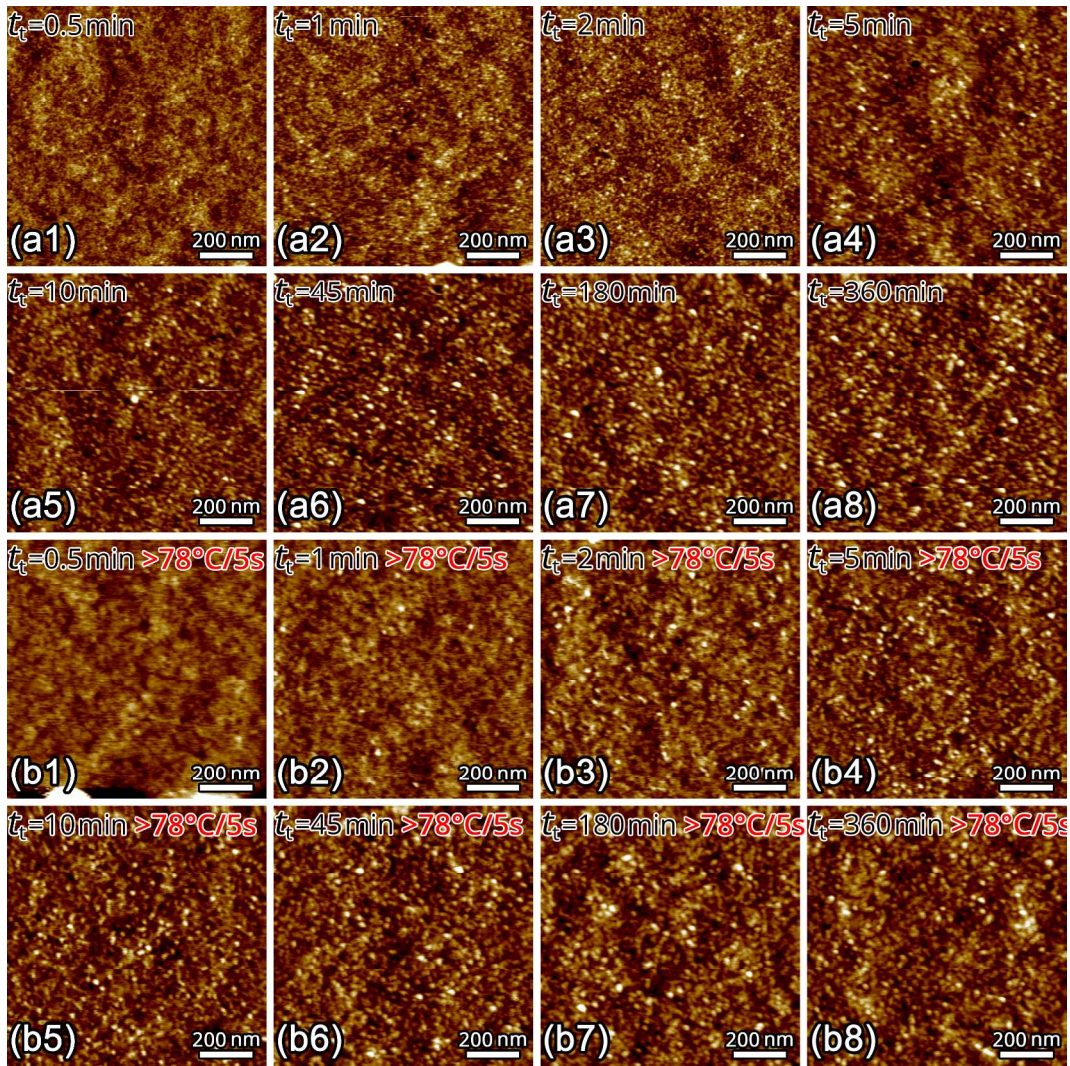


1
 2 **Figure S3.** FTIR spectra in the wavenumber range of 970–850 cm^{-1} for PLLA films that treated
 3 under 2 MPa CO_2 at $T_t = 0^\circ\text{C}$ for different $t_t = 0$ s (melt-quenched) (left) and $t_t = 30$ s (right), and
 4 then thermally annealed at $T_a = 80\text{--}135^\circ\text{C}$ for $t_a = 1$ min.



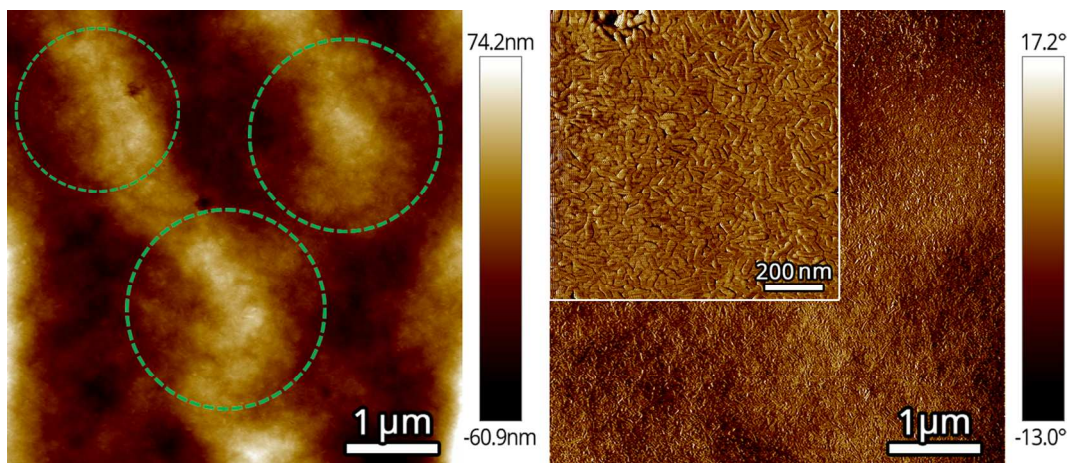
6
 7 **Figure S4.** POM (a–d) micrographs and AFM height (a1–d1) and phase (a2–d2) images for
 8 PLLA films that treated under 2 MPa CO_2 at $T_t = 0^\circ\text{C}$ for $t_t = 2$ min (a, a1, a2), $t_t = 10$ min (b, b1,
 9 b2), $t_t = 45$ min (c, c1, c2), $t_t = 180$ min (d, d1, d2), and then thermally annealed at $T_a = 130^\circ\text{C}$
 10 for $t_a = 1$ h.

11



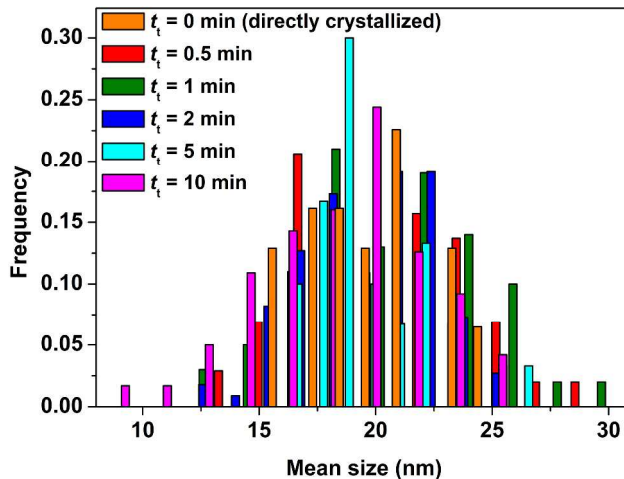
1
 2 **Figure S5.** AFM height images for CO₂-treated PLLA (mesophase) before (a1–a8) and after
 3 (b1–b8) annealing at $T_a = 78\text{ }^\circ\text{C}$ for $t_a = 5\text{ s}$. The CO₂ treatments were conducted at 2 MPa and T_t
 4 $= 0\text{ }^\circ\text{C}$ for different t_t (0.5–360 min) as indicated. After annealing, in contrast to the samples with
 5 $t_t = 5\text{--}360\text{ min}$ (b4–b8), whose morphologies remained substantially unchanged, a change in
 6 morphology can be seen in those with $t_t = 0.5\text{--}2\text{ min}$ (b1–b3), indicating that the samples with t_t
 7 $= 0.5\text{--}2\text{ min}$ had relatively low viscosity.

8



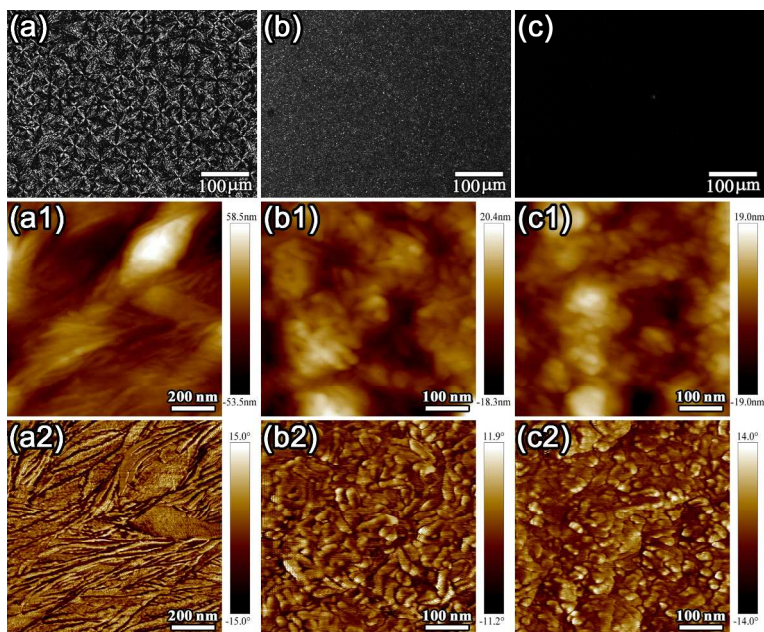
1
 2 **Figure S6.** AFM height (a) and phase (b) images for PLLA film that treated under 2 MPa CO₂ at
 3 $T_t = 0\text{ }^\circ\text{C}$ for $t_t = 2\text{ min}$ and then thermally annealed at $T_a = 130\text{ }^\circ\text{C}$ for $t_a = 1\text{ h}$. The dashed
 4 circles in panel (a) imply the grains observed in POM of Figure 4; the inset in panel (b) shows a
 5 high-magnification phase image.

6



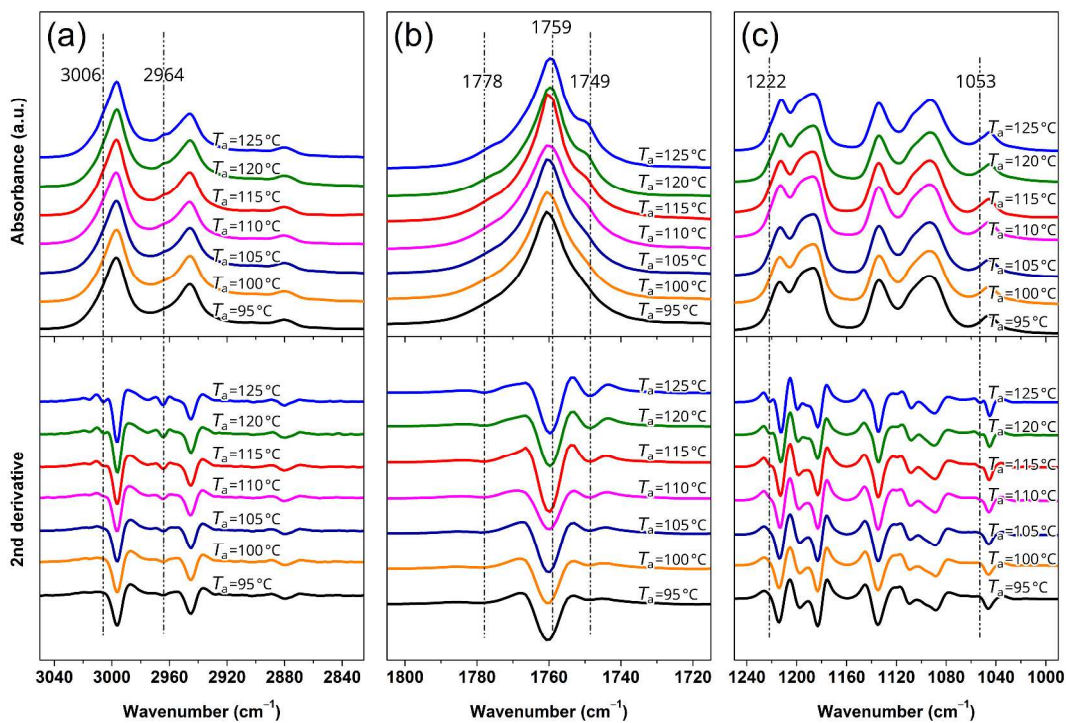
7
 8 **Figure S7.** The size distribution of lamellae (directly crystallized) and nanorods determined from
 9 the PLLA films that treated under 2 MPa CO₂ at $T_t = 0\text{ }^\circ\text{C}$ for different t_t (0.5–10 min) and then
 10 thermally annealed at $T_a = 130\text{ }^\circ\text{C}$ for $t_a = 1\text{ h}$.

11



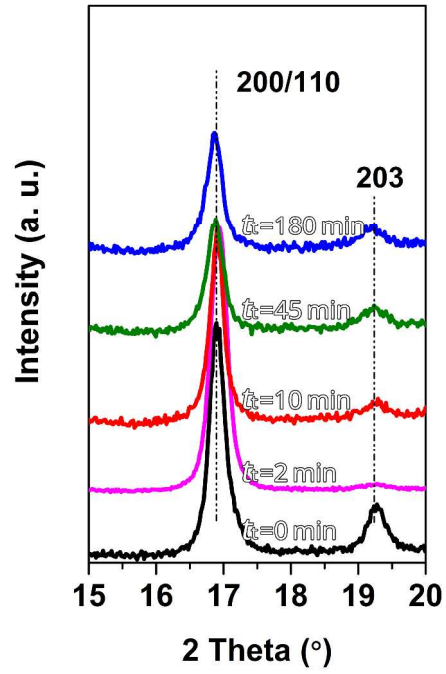
1
 2 **Figure S8.** POM (a–c) micrographs and AFM height (a1–c1) and phase (a2–c2) images for
 3 PLLA films that treated under 2 MPa CO₂ at $T_t = 0$ °C for $t_t = 2$ min (b, b1, b2) and $t_t = 10$ min (c,
 4 c1, c2), and then thermally annealed at $T_a = 90$ °C for $t_a = 1$ h. For comparison, panels (a, a1, a2)
 5 show the results for the sample that directly melt-crystallized at 90 °C (cooled from 210 °C).

6



1
 2 **Figure S9.** FTIR and corresponding second derivative spectra in the wavenumber ranges of
 3 3050–2850 (a), 1800–1720 (b), and 1250–1000 cm^{-1} (c) for PLLA samples that treated under 2
 4 MPa CO_2 at $T_t = 0\text{ }^\circ\text{C}$ for $t_t = 30\text{ min}$, and then thermally annealed at $T_a = 95\text{--}125\text{ }^\circ\text{C}$ for $t_a = 1\text{ h}$.

5
 6

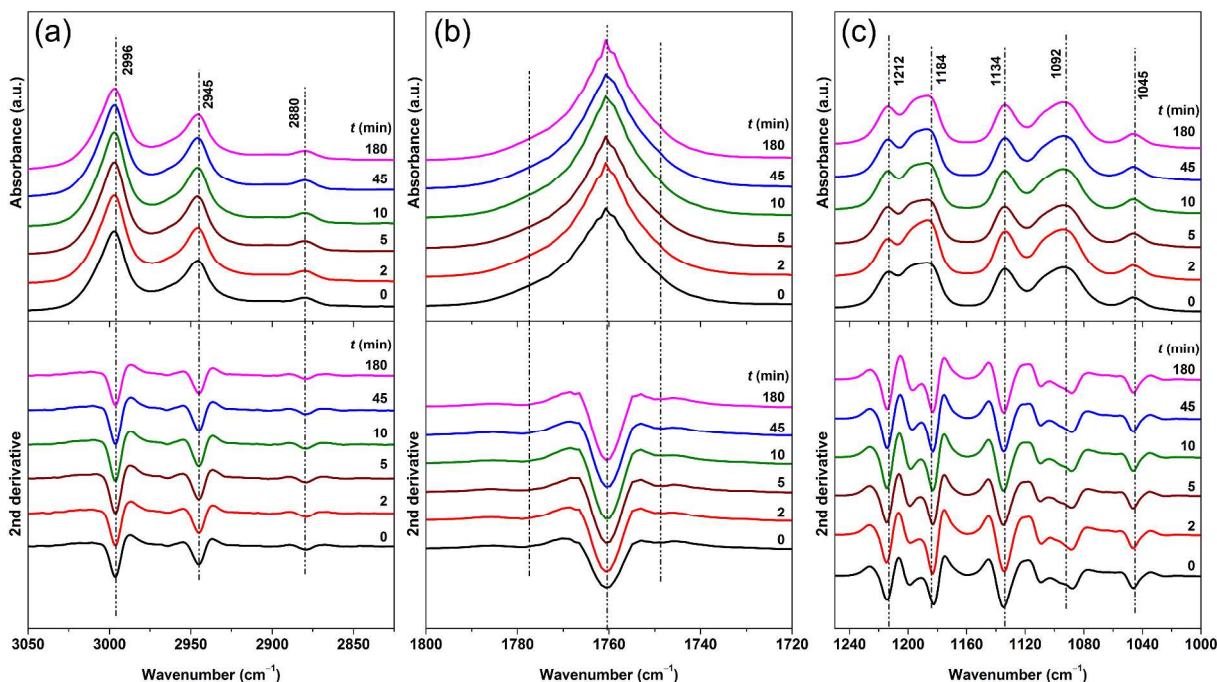


1

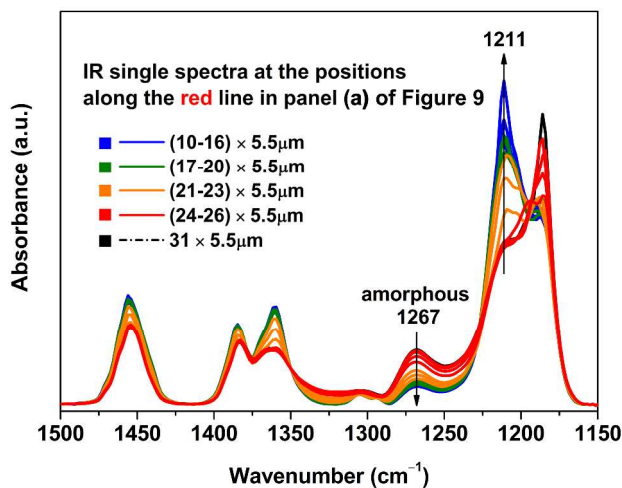
2 **Figure S10.** WAXD patterns for PLLA samples that treated under 2 MPa CO₂ at $T_t = 0$ °C for t_t
3 = 0–180 min (b), and then thermally annealed at $T_a = 130$ °C for $t_a = 1$ h.

4

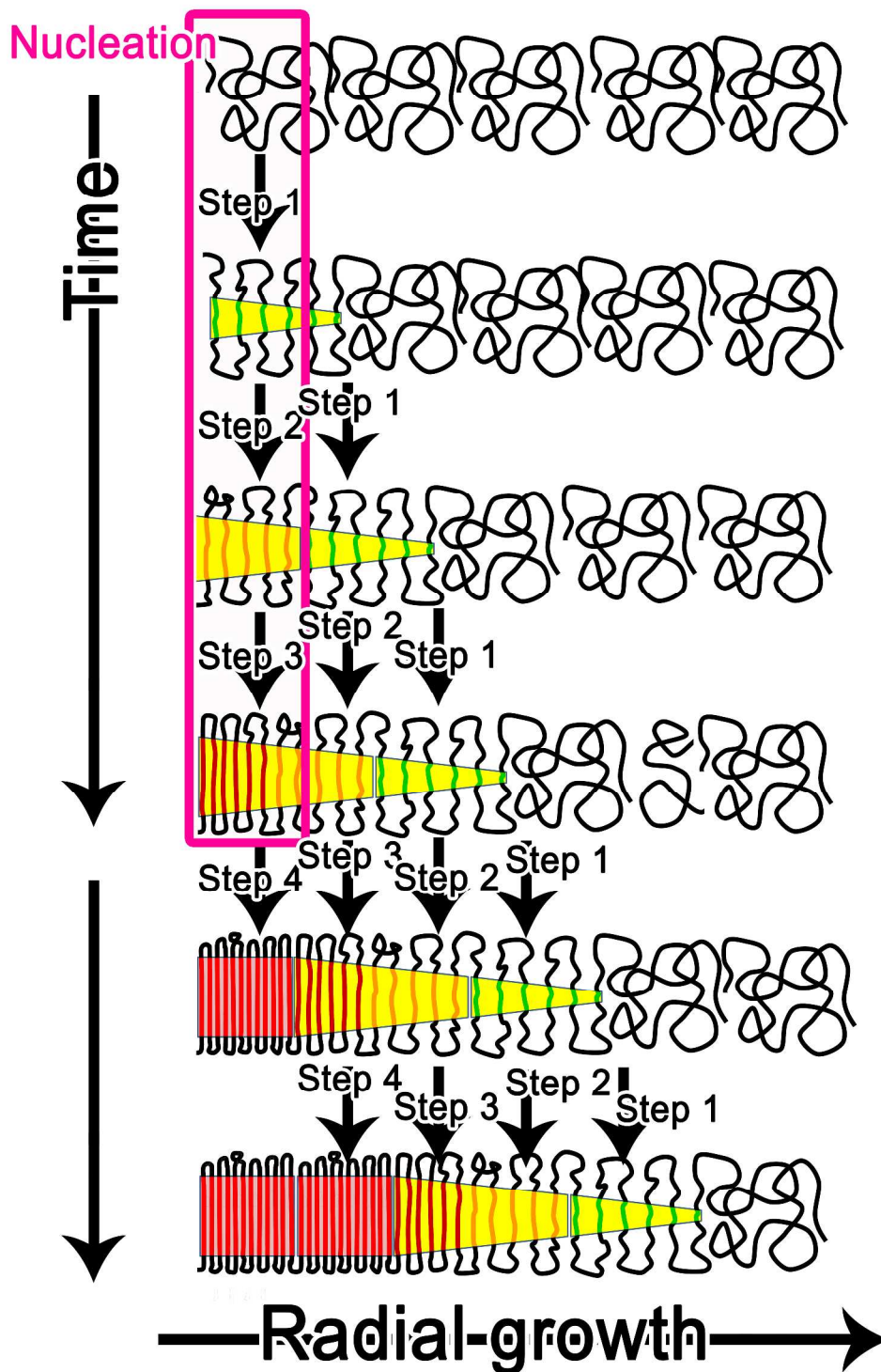
5



1
 2 **Figure S11.** FTIR and corresponding second derivative spectra in the wavenumber ranges of
 3 3050–2850 (a), 1800–1720 (b), and 1250–1000 cm^{-1} (c) for PLLA samples that treated under 2
 4 MPa CO_2 at $T_t = 0^\circ\text{C}$ for $t_t = 0$ –180 min as indicated, and then thermally annealed at $T_a = 90^\circ\text{C}$
 5 for $t_a = 1$ h.

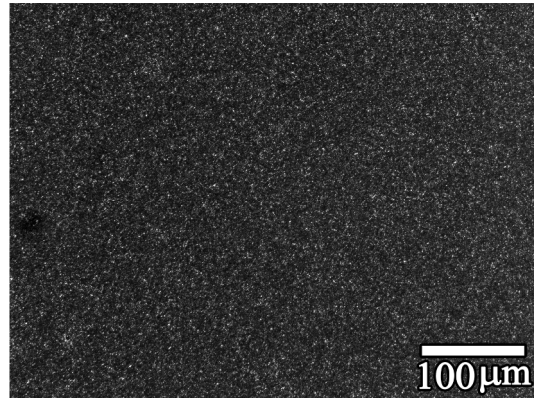


7
 8 **Figure S12.** FTIR spectra in the wavenumber range of 1500–1150 cm^{-1} at the positions marked
 9 along the red line in panel (a) in Figure 9.



1
 2 **Figure S13.** Schematic representation (replotted from Figure 10 for easier visualization) of
 3 multistage model proposed for the formation of the PLLA crystals (spherulites). The Steps 1-3
 4 represent the multistep nucleation process. The figure is not to scale.

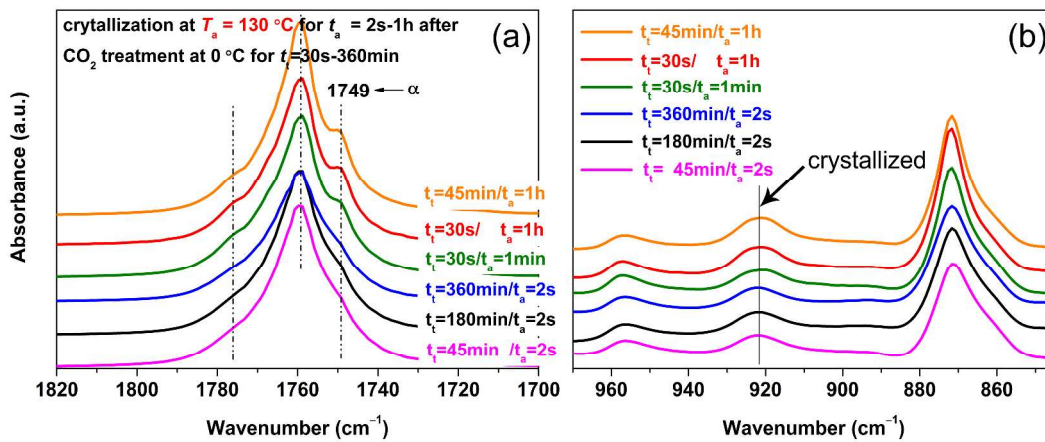
1



2

3 **Figure S14.** POM micrograph for PLLA film that treated under 2 MPa CO₂ at $T_t = 0$ °C for $t_t =$
4 30 s and then thermally annealed at $T_a = 130$ °C for $t_a = 1$ min.

5



6

7 **Figure S15.** FTIR spectra in the wavenumber ranges of (a) 1820-1700 and (b) 970–850 cm⁻¹ for
8 PLLA films that treated under 2 MPa CO₂ at $T_t = 0$ °C for different t_t as indicated and then
9 thermally annealed at $T_a = 130$ °C for $t_a = 2$ s–1 h as indicated.

10

11

12

13

1 **References**

- 2 (1) Zhang, T. P.; Hu, J.; Duan, Y. X.; Pi, F. W.; Zhang, J. M. Physical Aging Enhanced
3 Mesomorphic Structure in Melt-Quenched Poly(L-lactic acid). *J. Phys. Chem. B* **2011**, *115*,
4 13835–13841.
- 5 (2) Lan, Q. F.; Li, Y.; Chi, H. T. Highly Enhanced Mesophase Formation in Glassy Poly(L-
6 lactide) at Low Temperatures by Low-Pressure CO₂ That Provides Moderately Increased
7 Molecular Mobility. *Macromolecules* **2016**, *49*, 2262–2271.
- 8